Original Paper

Enhanced oil recovery with a thermo-thickening viscoelastic surfactant: A comparison with polymer

Mo-Yi Li [a], Quan Yin [a], Bo Li [b], Rui-Bo Cao [b], Yan Zhang [a], Xue-Zhi Zhao [a,*], Yu-Jun Feng [a,**]

[a] Polymer Research Institute, State Key Laboratory of Advanced Polymer Materials, Sichuan University, Chengdu, 610065, Sichuan,

63712, Heilongjiang, People0ûb

conditions. To address these challenges, a viscoelastic surfactant, 3-(*N*-erucamidopropyl-*N*,*N*-dimethyl ammonium) betaine (EDAB), was developed and systematically compared with HPAM. Experimental results demonstrate that EDAB outperforms HPAM in thermal resilience, salt tolerance, and interfacial activity. Unlike HPAM's thermal thinning behavior, EDAB displays thermo-thickening properties, with viscosity rising from 225 to 366 mPa□s as temperature increases from 25 to 55 °C. EDAB maintains 100% viscosity retention under 80 mg□L^{-1} Ca^{2+} or Mg^{2+}, whereas HPAM experiences 46% viscosity loss under identical ionic conditions. Core-flooding tests conducted under simulated Daqing oil reservoir conditions indicate that EDAB achieves a 1.4% higher incremental oil recovery factor than HPAM with equal initial solution concentration. When HPAM was employed as a mobility control for pre- or post-flush, EDAB elevates the recovery factor by 13.9% over water flooding. These comparative analyses underscore the potential of EDAB as a thermally stable, salt-insensitive alternative to HPAM, offering an optimized chemical strategy for EOR in challenging reservoir environments. The findings provide empirical validation for surfactant-based solutions to address HPAM's operational constraints in low-permeability formations.

I tro a tio

Approximately two thirds of the original oil in place still remain in reservoirs after conventional primary (self-flow by natural forces) and secondary (re-pressurization using water flooding in most cases) production (Lake et al., 1992; Sandrea and Sandrea, 2007; Jafarbeigi et al., 2022). Much of the residual oil could be further produced by the enhanced oil recovery (EOR) process (Thomas, 2008; Al-Asadi et al., 2023; Zamani et al., 2024), among which chemical flooding represents one of the most effective procedures, and has been most frequently employed in China (Chang et al., 2006).

Chemical flooding inv

However, from a chemical perspective, certain adverse interactions impede the success of SP modes in reservoirs with divalent cations. The predominant EOR polymer, high-molecular-weight partially hydrolyzed polyacrylamide (HPAM) (Chen et al., 2023; Seright and Wang, 2023), exhibits inherent limitations: susceptibility to viscoelastic degradation in brines containing Ca^{2+} and Mg^{2+} (Akstinat, 1980; Zaitoun and Poitie, 1983) and thermal instability under reservoir temperatures (Muller, 1981a, 1981b). Additionally, HPAM demonstrates pronounced mechanical vulnerability to irreversible shear-induced chain scission during flow through porous media (Seright, 1983; Chauveteau and Sorbie, 1991; Li et al., 2020), causing molecular weight reduction, polydispersity expansion, and consequent permanent viscosity loss.

Petroleum sulfonates and synthetic alkylaryl-sulfonates are preferred surfactants in SP formulations due to their cost-effectiveness and significant IFT reduction capabilities. However, their limited electrolyte stability, particularly against divalent cations in reservoir brines, presents operational constraints. Early studies (Bansal and Shah et al., 1978a, 1978b; Kumar et al., 1984) documented a concentration-dependent IFT elevation in petroleum sulfonate solutions when exposed to $CaCl_2$ or $MgCl_2$ in connate water. Agharazi-Dormani et al. (1990) further identified viscous precipitates formed through cation-surfactant interactions at ambient conditions. Such loss of IFT not only compromises interfacial activity essential for oil mobilization, but also exacerbates recovery challenges through viscosity degradation effects.

To obviate the above limitations of polymers and surfactants presently used, Lakatos et al. (2007) reported laboratory results of viscoelastic surfactant (VES) gel as mobility controlling agent in tertiary oil recovery. Such a gel is mainly composed of an alkyl-aryl sulfonate and the commodity nonionic surfactant ORS-64, achieving IFT reduction to 10^{-1} mN·m^{-1} magnitude. The gel demonstrated significantly enhanced resistance to thermal and shear degradation compared to conventional synthetic and natural polymer-based systems. Core flooding experiments demonstrated approximately 10% incremental oil recovery through simultaneous IFT reduction and mobility regulation, with potential improvements in microscopic displacement efficiency. Morvan et al. (2009) developed a viscoelastic surfactant (VES) fluid displaying viscosity-phase transitions at elevated temperatures and low surfactant concentrations in high-salinity brines (39,000 mg·L^{-1} TDS seawater or 20,000 mg·L^{-1} NaCl). The system exhibited brine-insensitive viscosity (3–15 mPa·s), 50 μg·g^{-1} surfactant adsorption in Clashach sandstone at 80 °C, and 29% incremental oil recovery over water flooding. However, the limited salt tolerance of these VESs, particularly toward multivalent cations, restricts its applicability to reservoirs in high total dissolved solids (TDS).

Xu et al. (2021) developed a novel Gemini VES (VES-Q) with erucyl amide tails and a cyclodextrin spacer. The bulky cyclodextrin group introduces steric hindrance, lowering the surfactant packing parameter (P) and reducing ion-induced dehydration. While VES-Q demonstrates stable viscosity (> 50 mPa·s) in high-salinity brines (Ca^{2+} or Mg^{2+} > 8000 mg·L^{-1})—outperforming conventional cationic VES systems—its practical use in high-temperature reservoirs remains limited due to its required high concentration and moderate thermal tolerance.

In contrast, Huang et al. (2022) designed a polyhydroxy cationic VES (SY-TO) with multiple hydroxyl groups in its hydrophilic head. This design strengthens the hydration layer, counteracting ion dehydration and maintaining stable wormlike micelles (WLMs) in extreme brines (> 14 wt% KCl or 10 wt% $CaCl_2$). Notably, SY-TO retains high viscosity (> 50 mPa·s) even at 140 °C, a property attributed to its dynamic aggregation-dissociation equilibrium under thermal molecular motion. These features position SY-TO as a promising candidate for fracturing in harsh reservoir conditions.

Microscopically, VES gels derive from entangled WLMs, flexible cylindrical aggregates formed by surfactant self-assembly above critical concentrations (Dreiss, 2007; Chu and Feng, 2011). These transient networks mimic polymer solutions, enabling broad applications (Yang, 2002). While conventional WLMs developed from cationic surfactants with hydrophobic tail less than C_{16} (Dreiss, 2007), recent advances focus on C_{22}-tailed cationic (Raghavan and Kaler, 2001; Croce et al., 2005) and zwitterionic (Kumar et al., 2007; Chu et al., 2010a, 2010b) surfactants, typically requiring salt or hydrotropic additives. Our prior work synthesized C_{22}-tailed anionic WLMs (Han et al., 2011) and ultra-long-chain amidosulfobetaines (Chu and Feng, 2009), revealing salt-free zwitterionic WLM formation and stimuli-responsive rheology (Chu et al., 2010; Chu and Feng, 2010a, 2010b, 2011). However, comparative advantages of VES over conventional HPAM polymers remain unverified, necessitating systematic evaluations under reservoir conditions. Very recently, we found a C_{22}-tailed betaine surfactant, 3-(*N*-erucamidopropyl-*N*,*N*-dimethyl ammonium) betaine (EDAB) exhibits a unique, abnormal thermo-thickening ability at 25–55 °C (Yin et al., 2022), which exactly falls in the typical oil reservoir temperature of Daqing Oilfield.

This study systematically compared EDAB with a conventional HPAM ($M_\eta = 1.2 \times 10^7$ g·mol^{-1}) regarding thickening ability, rheological behavior, IFT, long-term thermal stability, injectivity in porous media, as well as their ability to

at 45 °C after dehydration and degassing, was supplied by Daqing Oilfield.

2.2. Preparation of solutions

The solvent used is 4500 mg·L^{-1} NaCl synthetic brine to simulate the salinity of typical Daqing oil reservoir. A measured amount of EDAB or HPAM powder was added to the vortex of brine under agitation for 30 min. The resulting dispersions were then shaken for 24–36 h (100 rpm, 25 °C) to achieve homogeneous solutions, which were left overnight before measurement.

For the salinity resistance evaluation, the surfactant or polymer concentration remains fixed at 2000 mg·L^{-1}, while the salinity varies according to the experimental design. The dissolution procedure follows the same protocol as described earlier.

2.3. Rheological test

Rheological experiments were carried out on a Physica MCR 301 (Anton Paar, Austria) rotational rheometer at 45±0.1 °C, and a solvent trap was used to minimize water evaporation. A Searle-type concentric cylinder geometry CC27 (ISO3219) with measuring bob radius of 13.33 mm and measuring cup radius of 14.46 mm was applied for all the test.

The first normal stress differences (N_1) of solutions were measured using a Physica MCR 302 rheometer with a cone-and-plate geometry (50 mm diameter, 1° cone angle). Shear rate was incrementally increased from 1 up to 3000 s^{-1}.

To investigate the shear resistance of EDAB and HPAM, the specimens were sheared at 12,000 rpm for 60 s at room temperature using a mixing speed governor (WT-VSA2000B, China). Then, the apparent viscosity of the sheared solutions was measured at 45 °C after different resting times.

2.4. IFT measurement

The IFT between the sample solution and oil phase was measured using a TX500C interfacial tensiometer (CNG, USA). Prior to analysis, the measurement tube was sequentially cleaned with isopropanol and preconditioned through multiple rinses with the test solution. The tube was then filled with the sample solution, followed by precise injection of crude oil into its axial center using a microliter syringe. The tube was sealed and positioned in the instrument's measurement chamber, with care taken to prevent air bubble formation or oil adhesion to the tube walls. IFT values were calculated via digital droplet analysis, utilizing recorded dimensions (length and width) of the suspended oil droplet. Experimental parameters included: temperature maintained at 45 °C, rotational speed fixed at 5,000 rpm, and imaging intervals programmed at 1-min increments for the initial 30 min, transitioning to 3-min intervals thereafter.

2.5. Long-term thermal aging

Identical concentrations (2000 mg·L^{-1}) of EDAB and HPAM solutions were prepared in synthetic brine (4400 mg·L^{-1} NaCl, 50 mg·L^{-1} $CaCl_2$, 50 mg·L^{-1} $MgCl_2$, total salinity 4500 mg·L^{-1}) for long-term thermal stability monitoring. N_2 was bubbled into the solutions for 1 h to displace oxygen inside. The surfactant or polymer solution is distributed into a series of sample vials and stored in an oven at 45 °C. At regular intervals over a 60-d period, one vial from each group is removed and viscosity is monitored using the MCR rheometer described above.

2.6. Core flooding test

To evaluate the performance of EDAB and HPAM solutions, crude oil recovery experiments were conducted using the experimental setup described in Fig. 1. The experimental setup consisted of a nitrogen bottle, a syringe pump, a cylinder holding the displacing fluid, a core holder, and an effluent collector.

2.6.1. Basic parameters of the cores

Before conducting core flooding tests, the basic parameters of the core were determined. The length (L) and diameter (d) of the cores were measured, followed by vacuum drying at 45 °C to a constant weight m_0. The core was saturated with synthetic brine (4500 mg·L^{-1} NaCl) using ZB-IV vacuum pressurized saturation device (ETUSE, Changzhou, China). The core was first vacuumed in the vacuum pressurized saturation device for 12 h, followed by

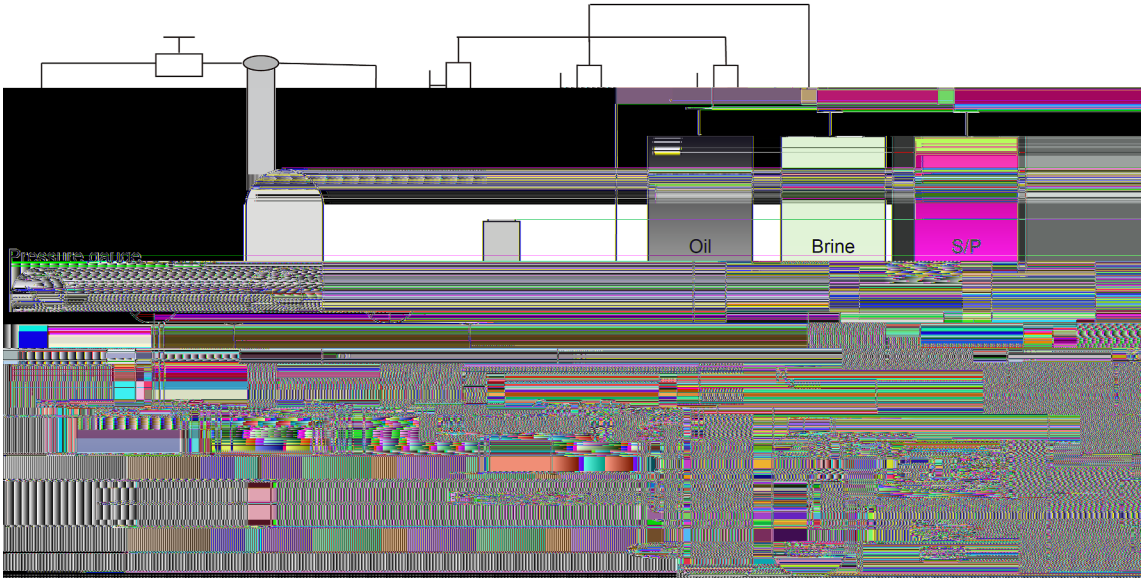

i Schematic diagram of core flooding test apparatus.

brine injection to initiate saturation. The saturation process lasted 12 h, with the pressure maintained at 10 MPa. The weight of the core was measured after saturation was completed and recorded as m_1, and then the pore volume (PV) and porosity (ϕ) of the core were calculated using the following equations:

$$\mathrm{PV} = \frac{m_1 - m_0}{\rho_w} \tag{1}$$

$$\phi = \frac{\mathrm{PV}}{\pi d^2 L / 4} \times 100\% \tag{2}$$

where ρ_w is the density of the brine, g·cm^{-3}.

2.6.2. Injectivity test

The brine-saturated core was placed into a core holder, with the confining pressure maintained at 4 MPa. The core was injected with synthetic brine (4500 mg·L^{-1} NaCl) for a certain period of time to keep the core saturated. While the temperature was increased to 45 °C until the inlet pressure was stabilized. Brine was injected at a rate of 0.2 mL·min^{-1}, the stabilized water flooding pressure was recorded, and permeability was calculated using Darcy's equation:

$$Q = K \frac{A \Delta P}{\eta L} \tag{3}$$

where η is the fluid viscosity, Pa·s; K is the

the concentration exceeds 2000 mg·L^{-1}, the thickening ability of HPAM significantly surpasses that of EDAB. This difference can be attributed to the formation of a WLMs network by EDAB at lower concentrations (Yin et al., 2022), which closely resembles the entangled network of HPAM molecular chains. At higher concentrations, HPAM can entangle to form a denser network. While EDAB also forms longer WLMs at high concentrations, the dynamic equilibrium of "breakage-reformation" within these micelles leads to lower viscosity than HPAM. The thickening ability of HPAM and EDAB can be delineated at 2000 mg·L^{-1}. Considering the requirements of practical use for low concentration and high viscosity, we ultimately selected 2000 mg·L^{-1} of both HPAM and EDAB for subsequent experiments. At this concentration, the apparent viscosity of the HPAM and EDAB solutions is 37 and 41 mPa·s, respectively.

3.1.2. Effect of salinity and divalent cations

Generally, the connate formation water of oil reservoirs contains Na^+ and multivalent cations like Ca^{2+} and Mg^{2+}, which shield electrostatic repulsion among the carboxylate groups along HPAM skeleton, causing collapse and aggregation of polymer chains, reducing hydrodynamic volume of polymer coil and lowering viscosity of polymer solution (Iyer et al., 2021). For instance, HPAM with a molecular weight of 15 million Dalton loses mor than 80% of its apparent viscosity in 10,000 mg·L^{-1} NaCl, undermining its efficiency to improve mobility ratio thus impairing its ability to enhance oil recovery (Li, 2015). Therefore, it is an indispensable to examine the impact of salinity and polyvalent cations on viscosity buildup of any chemicals used for EOR process.

First, the effect of Na^+ on the thickening ability of HPAM and EDAB was investigated. As shown in Fig. 3(a), with elevation of NaCl concentration from 0 to 4500 mg·L^{-1}, the apparent viscosity of the HPAM solution at 2000 mg·L^{-1} decreases sharply, from 326.0 to 33.8 mPa·s, with 89.6% of loss in viscosity. This is attributed to the weakening of electrostatic interactions between HPAM molecular chains as the NaCl concentration increases. When further increasing NaCl concentration to 15,000 mg·L^{-1}, the decrease in viscosity slowed down significantly from 33.8 to 19.3 mPa·s, which was only 4.4%. This indicates that the electrostatic shielding effect of NaCl on the HPAM molecular chains gradually approaches saturation, causing the viscosity to stabilize.

On the contrary, within the whole salinity investigated (from 0 to 15,000 mg·L^{-1} NaCl), the apparent viscosity of EDAB solution remains unchanged, always at 41 mPa·s irrespective of the salinity. As a betaine surfactant, the stoichiometric cationic and anionic groups in EDAB attract electrostatically; when NaCl is introduced, such an attraction is shielded by both Na^+ and Cl^-, making the headgroups aggregate together; in other words, the EDAB molecules are readily assembling into wormlike micelles, showing strong thickening ability macroscopically.

Furthermore, the effect of divalent cations on the apparent viscosity of HPAM and EDAB solutions was examined. As exhibited in Fig. 3(b), the apparent viscosity of the EDAB solution remains almost unchanged whatever the alteration of Ca^{2+} and Mg^{2+}, stabilizing at around 41 mPa·s. This indicates that divalent cations do not affect the thickening ability of EDAB solution, as these cations cannot be complexed with carboxylate groups in EDAB molecule, owing to the stoichiometric attraction between positive ammonium and negative carboxylate.

In contrast, low concentrations (0–10 mg·L^{-1}) of Ca^{2+} and Mg^{2+} initially increase the viscosity of the HPAM solution, while further increases in their concentration leads to a significant decrease in viscosity. When the concentration of Ca^{2+} and Mg^{2+} reaches 80 mg·L^{-1}, the viscosity of the HPAM solution drops to 21.6 mPa·s, with a viscosity retention (R_η, percentage of changed viscosity relative to initial viscosity) of 63.5%. The reduction in viscosity at high concentration of Ca^{2+} and Mg^{2+} is related to electrostatic shielding, whereas the increase in viscosity at low dosage may be attributed to weak complexation among these divalent cations and carboxylate groups along HPAM main chains (Pu et al., 2016). As the divalent cations Ca^{2+} and Mg^{2+} can simultaneously create electrostatic attractions with two carboxylate groups on the HPAM molecular chains, resulting in weak cross-linking between the chains and thereby enhancing the viscosity of the solution.

3.1.3. Effect of temperature

The change in temperature from surface to bottomhole, from borehole to reservoir, will also significantly affects the performance of chemicals used in EOR process (Belhaj et al., 2020). Therefore, we further investigated the impact of temperature on the apparent viscosity of HPAM and EDAB solutions.

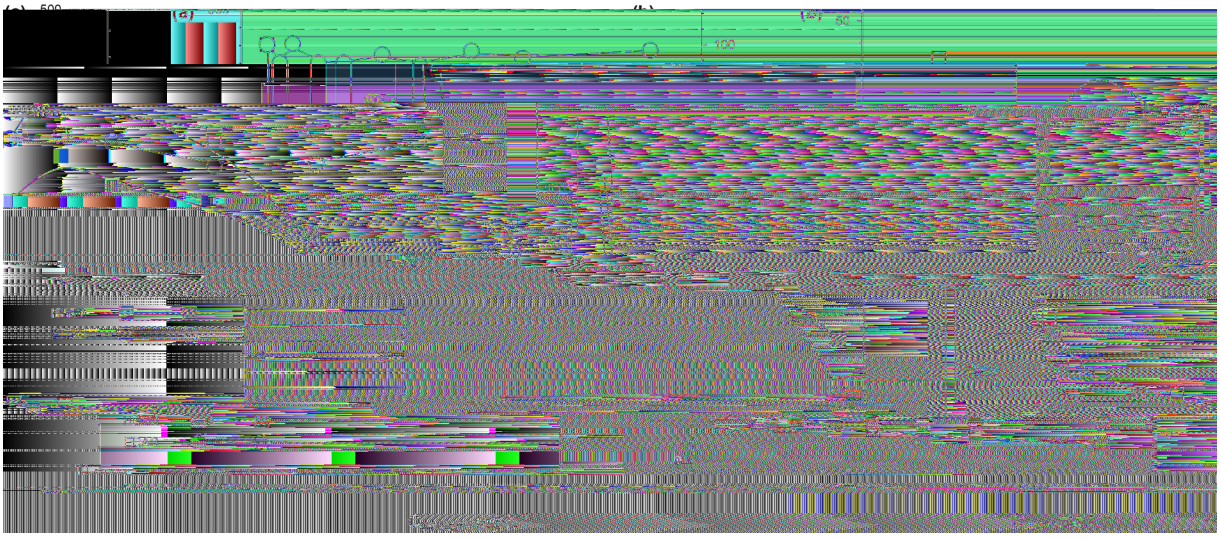

Fig. 4 shows the apparent viscosity profile of 2000 mg·L^{-1} EDAB and HPAM solutions in the temperature range of 20–80 °C. One can find that the viscosity of the HPAM solution decreases gradually with increasing temperature, exhibiting typical "thermo-thinning" phenomenon, as always evidenced in the literature results (Yang, 2001). When the temperature rises from 25 to 45 °C, the viscosity decreases from 41 to 33 mPa·s, resulting in a viscosity retention rate of 80.5%. Further increasing the temperature to 80 °C results in a final viscosity of 22 mPa·s, with a viscosity retention rate of only 53.7%.

In contrast, the viscosity of the EDAB solution initially increases with rising temperature before subsequently decreasing, demonstrating a "thermally thickening" behavior. At 25 °C, the viscosity of the EDAB solution is 28 mPa·s, then increases to 37 mPa·s at 45 °C, marking 32.1% of enhancement. Upon further heating to 55 °C, the viscosity peaks at 53 mPa·s, with an increase of 89.3%. However, at 80 °C, the viscosity drops to 15 mPa·s, with a viscosity retention rate of 53.5%, which is very close to that of HPAM. The thermo-thinning of the HPAM solution is attributed to the dehydration-induced coiling of the polymer chains at high temperatures (Gao, 2013), while the thermally thickening behavior of EDAB is due to the increased persistence length (l_p) of the WLMs within the solution (Yin et al., 2022). The sharp viscosity decrease in EDAB solutions above 55 °C occurs because the persistence length of its wormlike micelles—after initially increasing with temperature—declines rapidly beyond this point (Yin et al., 2022). This persistence length reduction diminishes micellar rigidity and hydrodynamic volume, lowering viscosity. Similar behavior has been reported in studies of wormlike micelles by Zhang et al. (2015) and Raghavan and Kaler (2001). Therefore, from the viscosity–temperature curve, EDAB shows superior thermal stability at around 45 °C (Daqing oil reservoir temperature), highlighting its potential for application under this reservoir condition.

3.2. Rheological behavior of EDAB and HPAM solutions

During practical applications such as dissolution, dispersion, and pumping, the polymer molecules in displacing fluid are subjected to varying degrees of shear. In low to medium permeability oil reservoirs, these solutions also experience significant shear and elongation when flowing through porous media (Lai et al., 2016). Therefore, we compared the rheological behavior of HPAM and EDAB solutions.

3.2.1. Shear-thinning behavior

Fig. 5 indicates the flow curves of 2000 mg·L^{-1} EDAB and HPAM solutions. One can immediately find that both curves can be divided into three parts: Newtonian plateau at low shear rate region, shear-thinning slope at intermediate shear rate regime, and a second Newtonian plateau at high shear rate. More importantly, both curves can be fitted perfectly with the classical Carreau model (in set of Fig. 5). However, there are also some differences between two solutions. First, the first critical shear rate ($\dot{\gamma}_1^*$) of EDAB solution (0.003 s^{-1}) at which Newtonian plateau transits to shear thinning appears one order of magnitude earlier than that of HPAM solution (0.025 s^{-1}). This is understandable, as the physical supramolecular aggregates self-assembled from small surfactant molecules are more readily ruptured than the entanglements of long HPAM chains. The second difference comes from the shear-thinning degree of the solution; that is, the degree of viscosity reduction over a range of shear rate intervals, which can be quantitatively characterized by the power-law index, n, of the Carreau equation. EDAB solutions exhibit pronounced shear-thinning behavior, meaning their viscosity decreases more significantly under shear compared to their resting state. This property offers practical advantages: easier pumping and injection from the surface to the wellbore with reduced power requirements, and improved flow through reservoir pore throats, where shear-induced disassembly of worm-like assemblies prevents blockages and enhances deeper penetration. The third difference comes from the second critical shear rate ($\dot{\gamma}_2^*$), which is the junction between the shear-thinning region and the second Newtonian plateau region, above which the viscosity of both solutions decreases to about 6 mPa·s and remains constant; in other words, even if the assemblies are disassembled, the 2000 mg·L^{-1} EDAB solution still has the ability to regulate the flow. It is noteworthy, however, that $\dot{\gamma}_2^*$ of EDAB (215 s^{-1}) still appeared a bit

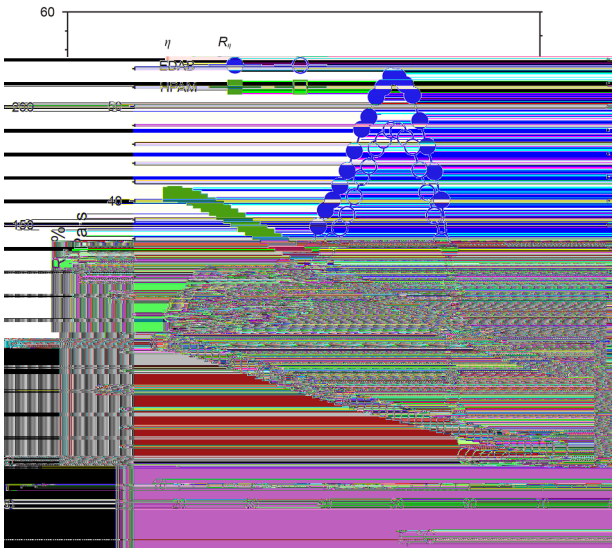

i Apparent viscosity of 2000 mg·L^{-1} EDAB and HPAM solutions plotted as a function of temperature. TDS, 4500 mg·L^{-1} NaCl; $\dot{\gamma}$, 10 s^{-1}.

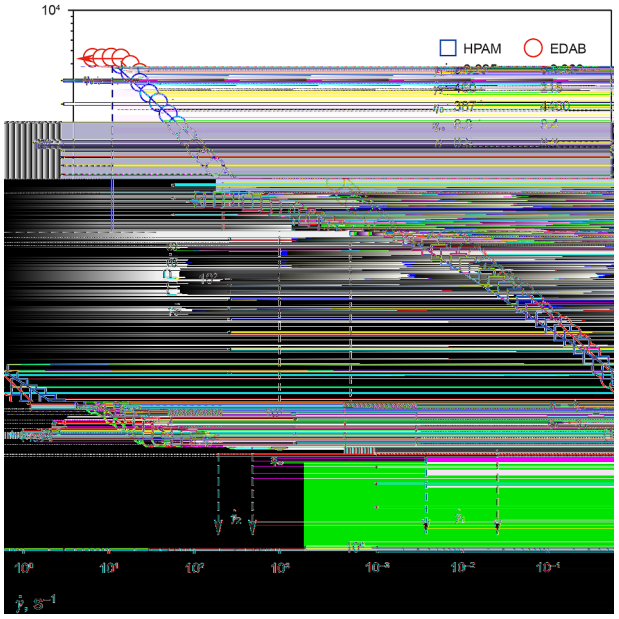

i **5** Steady viscosity of 2000 mg·L^{-1} EDAB and HPAM solution as a function of shear rate. TDS, 4500 mg·L^{-1} NaCl; T, 45 °C. Solid lines represent Carreau model fits, where η

earlier than that of HPAM (460 s^{-1}), but the gap narrowed to a factor of two.

We further compared the shear resistance of EDAB and HPAM solutions through shear degradation tests. As shown in Fig. S1, after 60 s of shearing at 12,000 rpm, the viscosity (41 mPa·s) of the 2000 mg·L^{-1} EDAB solution remained almost unchanged, with 100% viscosity retention rate. However, for the same concentration of HPAM solution, the viscosity decreased from the initial value (36 mPa·s) to 20.5 mPa·s after high-speed shear and its viscosity retention rate was only 56.9%. This observation suggests that the surfactant EDAB has better resistance to shear degradation than the polymer HPAM.

3.2.2. The first normal force

As current research demonstrates, the elastic properties of displacing fluids play a significant role in enhanced oil recovery (Wang et al., 2000). Zhong et al. (2022) established that these elastic effects substantially influence the viscosity of displaced phases. Furthermore, viscoelasticity has been shown to improve microscopic displacement efficiency (Ameli et al., 2019), with viscoelastic fluids finding widespread application in oilfield development (Masuda et al., 1992; Zeynalli et al., 2023; Xue et al., 2024). These findings underscore the importance of investigating the viscoelastic properties of both EDAB and HPAM solutions. However, the tiny elasticity of dilute solution cannot be determined from elastic modulus (Fig. S2). Therefore, the first normal stress difference (N_1), the difference between the principal stress and the stress at its vertical direction (as illustrated in Fig. S3), was selected here to quantitatively describe the viscoelasticity of EDAB and HPAM solutions within a shear rate range of 1–3000 s^{-1}.

As displayed in Fig. 6, with increasing shear rate, N_1 of both EDAB and HPAM solutions initially remains constant when the shear rate is less than 10 and 40 s^{-1}, indicating that the micellar structure in the EDAB solution is disrupted under lower stress, leading to a loss in viscosity. It is noteworthy that the N_1 of the EDAB solution begins to rise at a shear rate of 10 s^{-1}, which aligns with the shear rates typically encountered in actual oil displacement processes. Furthermore, the N_1 of the EDAB solution is greater than that of the HPAM solution, suggesting that during the actual displacement process, the EDAB solution exhibits better viscoelasticity. The characteristic correlation constant ψ of the material and the exponent of the effect of shear rate on stress m can be obtained from the fitting of the experimental data. EDAB has a higher value of ψ (0.48) and a larger value of m (0.88), which indicates that EDAB exhibits a stronger stress enhancement effect during the flow process. Whereas, HPAM has a lower value of ψ (0.22) and a smaller value of m (0.71), indicating that it is less viscoelastic.

Additionally, when the shear rate exceeds the critical value, N_1 for both the EDAB and HPAM solutions begins to increase. At this point, the relaxation time (τ_R) of the solution can be described by the following equation (Zilz et al., 2014):

$$\tau_R = \frac{\psi}{2\eta_0} \tag{7}$$

where ψ is a constant; and η_0 represents the zero-shear viscosity of the solution. Based on Eq. (7), the relaxation time of 2000 mg·L^{-1} EDAB and HPAM solutions calculated is 0.54 and 0.28 s, respectively. The longer relaxation time for EDAB solution indicates that it possesses stronger elasticity compared to the HPAM solution.

3.3. Dynamic IFT

Reduction in IFT between oil and water phases is one of the key mechanisms for surfactant EOR (Ahmed et al., 2023). Therefore, the ability of EDAB to lower IFT was investigated in comparison with HPAM.

As depicted in Fig. 7(a), the IFT between HPAM aqueous solution and Daqing oil remains in the order of 10^1 mN·m^{-1} across all tested concentrations, while EDAB can significantly
to the order of 10^{-2} mN·m^{-1}. Such a difference is attributed to the non-amphiphilic of HPAM, which prevents it from adsorbing at the oil/water interface. In contrast, EDAB, as a typical zwitterionic surfactant, can effectively adsorb at the oil/water interface, leading

when the concentration of EDAB is 1000 mg·L^{-1}, the oil/water IFT drops to 8 × 10^{-2} mN·m^{-1}, whereas the IFT the equivalent concentration of AM solution remains at .5 × 10^1 mN·m^{-1}. While most surfactants employed in the Daqing oilfield are known to achieve ultra-low IFT (< 10^{-3} mN·m^{-1}) (Chen et al., 2018; Sun et al., 2018; Liu et al., 2024), EDAB may not match their interfacial activity. However, EDAB offers a distinct advantage: its unique thermal viscosity-enhancing capability, which these entional surfactants lack.

As surfactant and polymer are often mixed practically in binary chemical flooding, the interfacial activity of the mixture of EDAB and HPAM at different concentrations was also examined. The IFT of the ed decreases initially with ingzi O F yp-f dgfl9lte

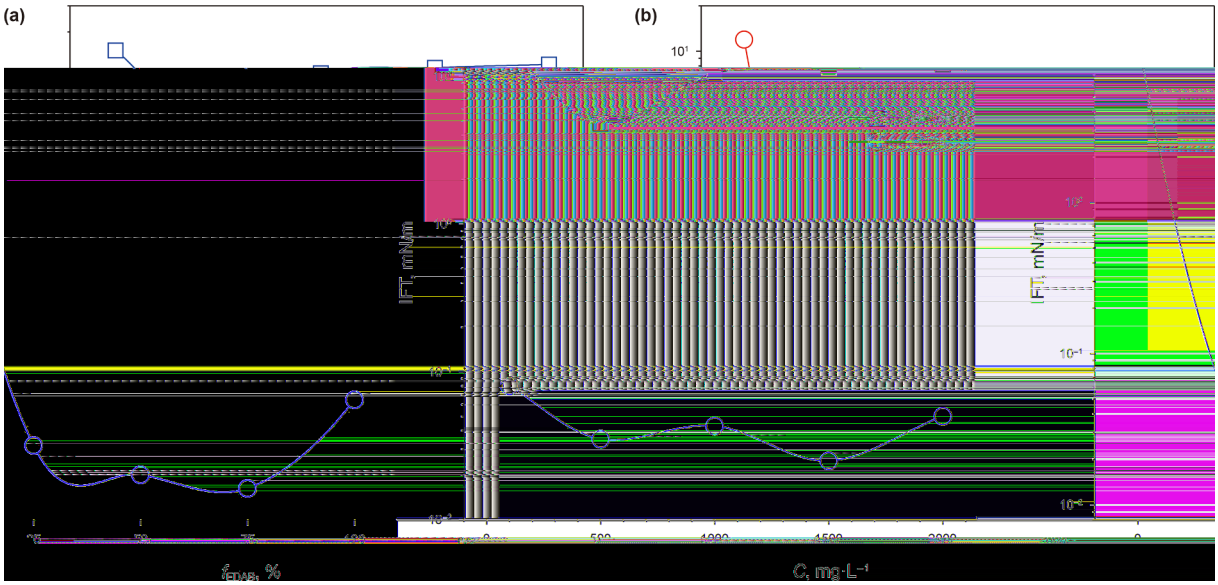

i IFT plotted as a function of EDAB or HPAM concentration at 45 °C. ( ) Variation of IFT with concentration of EDAB and HPAM; (**t**) the effect of EDAB mass fraction (f_{EDAB}) on IFT of mixture of HPAM and EDAB at the fixed total concentration of 2000 mg·L^{-1}. The TDS is 4500 mg·L^{-1}.

effects (Meng et al., 2024). As a result, the IFT in the EDAB/HPAM mixed system is lower than in solutions containing EDAB alone.

3.4. Long-term thermal stability

During the displacement processes, the displacing fluid normally experiences more than six months of the transportation at the reservoir temperature. Therefore, the long-term thermal stability represents one of the most important criteria for screening chemicals for EOR use. Therefore, the long-term stability of HPAM and EDAB under simulated reservoir temperature and salinity was monitored for their effectiveness in enhancing oil recovery.

Fig. 8 shows the decay of viscosity, as well as viscosity retention of both HPAM and EDAB solutions at 45 °C and different time intervals. One can find that at the first 30 d, the viscosity of the HPAM solution significantly decreased from 36 to 18 mPa·s, with a viscosity retention of 50%. Then, at another 30-d period, the viscosity remained relatively constant. In contrast, the viscosity of the EDAB solution remained completely unchanged throughout the 60 d of aging period, holding the initial viscosity of 41 mPa·s, with a viscosity retention of 100%. This indicates that, compared to the conventional HPAM, the surfactant EDAB exhibits exceptional long-term thermal stability. During the aging process, the molecular chains of HPAM undergo thermal degradation in the saline solution, leading to a reduction in molecular weight and, consequently, a substantial decrease in solution viscosity (Doe et al., 1987). Conversely, the WLMs formed by EDAB do not experience thermal hydrolysis, which allows the viscosity of the solution to remain unchanged.

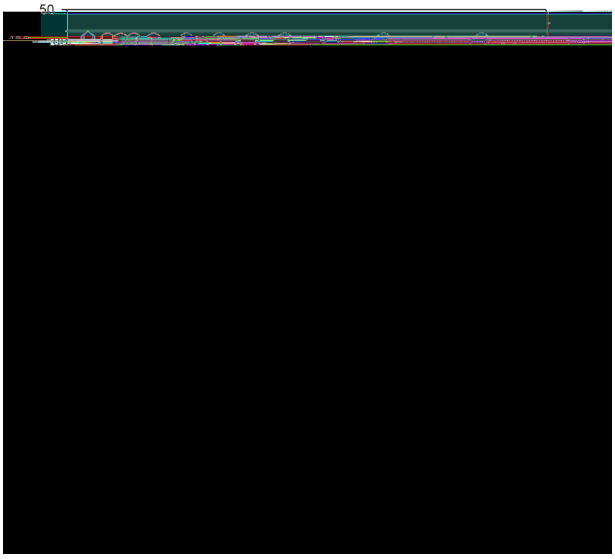

i 8 Apparent viscosity (η) and viscosity retention (R_η) plotted as a function of aging time (t) for 2000 mg·L^{-1} EDAB and HPAM solutions. $\dot{\gamma}$, 10 s^{-1}; TDS, 4500 mg·L^{-1}; T, 45 °C.

In summary, the comparison results between HPAM and EDAB suggest that HPAM exhibits slightly better thickening ability; however, EDAB significantly outperforms HPAM in terms of salt tolerance, IFT reduction, and long-term stability. However, the performance difference between the two in the actual oil displacement process still needs to be investigated. Therefore, the following core flooding experiments will be carried out at simulated oil reservoir condition of Daqing Oilfield (45 °C, 4500 mg·L^{-1} NaCl). These experiments will compare the injectivity and oil recovery factor at both equal concentration (2000 mg·L^{-1}) and equal apparent viscosity (24 mPa·s) for HPAM and EDAB, as well as mixed solution of both (C_{HPAM}: $C_{EDAB} = 1:1$, $\eta = 23$ mPa·s) at total concentration of 2000 mg·L^{-1}.

3.5. Core flooding

The injectability of the displacing fluid is crucial in determining its success in EOR process (Seright et al., 2009). Therefore, the propagation of HPAM and EDAB solutions in the cores were firstly evaluated. Fig. 9 shows the flow curves of 2000 mg·L^{-1} HPAM and EDAB solutions in the cores. It can be observed that both flow curves exhibit three distinct platforms, corresponding to the stable pressure during water flooding, HPAM or EDAB flooding, and subsequent water flooding. As the polymer or surfactant solution is injected, some pore spaces in the core are blocked by polymer

molecules or surfactant-formed micelles, causing the pressure to rise. As the injection volume increases, the injection pressure reaches its maximum and stabilizes, indicating that the polymer or surfactant solution can flow steadily through the core without plugging.

The core parameters used as well as the resistance factor (RF) and the residual resistance factor (RRF) calculated from Eqs. (3) and (4) are summarized in Table 1. The former is used to describe the reduction in oil/water mobility ratio and core permeability before and after the injection of the displacement fluid. Generally, a higher RF value implies greater flow resistance in the porous medium, which helps to expand the swept volume. The magnitude of RRF can be used to assess the ability of the displacing fluid to enhance oil recovery. However, excessively high RRF values may indicate that the displacing fluid is prone to blocking the porous medium (Zhu et al., 2022).

It can be observed that the RF (27.8) and the RRF (16.1) of the 2000 mg·L^{-1} HPAM solution are higher than those (RF, 19; RRF, 13.5) of the EDAB solution at the same concentration. This suggests that HPAM causes more significant blocking of the pore spaces during its flow through the core, resulting in greater retention inside the pores, which is beneficial for improving sweep efficiency. However, the viscosity of the 2000 mg–

during the water flooding stage, the recovery factor gradually increases with the injection volume until it stabilizes at 56.2%, at which point water flooding is stopped. In the chemical flooding stage, the 0.5 PV of HPAM solution injected into the core results in a gradual increase in pressure and a slight rise in recovery factor. Finally, during the subsequent water flooding stage, flooding pressure begins to decline, and the recovery factor increases, stabilizing at 68.3%. The net recovery factor by HPAM is the difference between total recovery factor and that by water flooding, that is, 12.1% of the recovery factor.

Under the same conditions, three core flooding tests were conducted with EDAB solution to verify experimental reproducibility. As shown in Figs. 10(a) and S4, the oil recovery factors of EDAB were measured as 11.1%, 11.3%, and 10.9% respectively, yielding an average recovery factor of 11.1%, which is 1% lower than that of HPAM. Table S1 lists the relevant parameters and experimental data of the core samples used in the replicate experiments. As indicated in Fig. 4, the thermal thickening ability of EDAB renders significantly higher viscosity at 45 °C compared to 25 °C, suggesting that EDAB should have a higher sweep efficiency. However, the low concentration of the EDAB solution used may result in a dilution that is not resistant to pre- and post-water flooding. This reduces the effective concentration of EDAB, diminishing the viscosity increase and lowering the sweep efficiency, which ultimately results in a lower recovery factor. Additionally, rcKlyp "P

preserves the thermal thickening effect of EDAB. The water flooding stage yielded a recovery factor of 59.0%, with EDAB contributing an additional 13.9%, bringing the total to 72.9%. Compared to EDAB injection without protective slugs, the slug-assisted method improved recovery by 2.7% and outperformed HPAM. This enhancement likely stems from reduced fluid dilution (due to the HPAM slugs) and higher viscosity of EDAB, which improves sweep efficiency and ultimately boosts recovery.

Additionally, we further investigated the difference in oil recovery efficiency between EDAB and HPAM solutions at same viscosity (Fig. 10(c)), with the corresponding parameters listed in Table 3 for Cores 5, and 6, respectively. As observed, the recovery factor from HPAM and EDAB are 7.3% and 8.7%, respectively, with EDAB showing a 1.5% higher than that by HPAM. This is because, at the same viscosity, the EDAB solution exhibits higher interfacial activity than the HPAM solution, significantly reducing the IFT (as shown in Fig. 7(a)). This reduction in IFT greatly diminishes the capillary effect in the formation, improving the displacement efficiency and resulting in a higher recovery factor.

Furthermore, we examined the oil recovery factor by the mixture solution of EDAB and HPAM as a SP binary flooding system (Fig. 10(d)). The core parameters (Core 8) used are shown in Table 3. The total concentration of the system was fixed at 2000 mg·L^{-1}, with an EDAB to HPAM mass ratio of 1:1. The IFT of the SP binary system was reduced to the order of 10^{-2} mN·m^{-1} (Fig. 7), and the viscosity was approximately 23 mPa·s. Notably, the HPAM-EDAB mixture exhibits lower thickening capability compared to single-component solutions at equivalent concentrations. This behavior likely stems from competitive solvation effects: EDAB's zwitterionic headgroups form strong interactions with water molecules, potentially limiting HPAM's access to hydration layers. Consequently, the reduced solvation of HPAM chains increases their rigidity, ultimately diminishing the solution viscosity. However, the recovery factor achieved by the SP binary system was 9.5%, which is higher than that of single EDAB and HPAM slug. This improvement can be attributed to the synergistic effect in the binary system: the surfactant EDAB reduces the oil–water IFT, while HPAM ensures the viscosity of the flooding fluid. As a result, the binary system exhibits both a large sweep efficiency and low IFT, leading to enhanced oil recovery.

However, it should be noted that during the initial water injection phase, all experimental groups exhibited smooth and consistent pressure curves with minimal fluctuation (Fig. 10). Through rigorous re-examination, we conclude that the characteristically flat and stable pressure profiles observed during initial waterflooding can be primarily ascribed to two interconnected factors: the rapid breakthrough dynamics and diminished pressure differentials inherent to the 8-cm short core samples employed in this study, and the inadequate resolution (0.04 MPa) of the pressure transducers, which falls below the threshold required for capturing such subtle transient variations.

Consequently, we subsequently implemented a comparative analysis of the oil displacement efficiencies of EDAB and HPAM solutions at the equal concentration (2000 mg·L^{-1}) using standardized 30-cm Berea cores, monitored with pressure transducers of significantly enhanced precision (0.01 MPa resolution). The comprehensive petrophysical properties of the Berea cores and the corresponding core flooding experimental results are recorded in Table 4. The experimental results demonstrate that during core flooding tests using EDAB solution on long core samples, the breakthrough pressure and stabilized pressure recorded in the initial water flooding stage were 0.25 and 0.22 MPa, respectively (as shown in Fig. 11). Corresponding measurements for HPAM solution flooding yielded breakthrough and stabilized pressures of 0.30 and 0.24 MPa. This indicates minimal differentials between breakthrough and stabilized pressures ($\Delta P \leq 0.06$ MPa) during water flooding in Berea cores. Consequently, when employing short core samples where transient pressure dynamics occur within sub-detection timescales, the virtual absence of measurable differences between breakthrough and stabilized pressures becomes scientifically plausible.

For the EDAB system in long-core water flooding, the oil recovery factor progressively increased with the injection volume of brine until stabilizing at 49.4%. During the chemical flooding phase, following the injection of 0.5 PV of EDAB solution, the displacement pressure demonstrated a systematic buildup. Subsequent post-water injection triggered a gradual pressure decline while progressively enhancing oil recovery, ultimately stabilizing at 60.0%. Consequently, EDAB delivered a quantifiable

Summary of oil recovery factors for validation experiments using Berea cores.

Core No.	Displacing fluid	η_1, mPa·s	η_2, mPa·s	L, cm	l, cm	PV, cm^3	ϕ, %	K_w, mD	E_w, %	$E_{p(s)}$, %	E_T, %
11	EDAB	28	37	30.0	4.5	86.5	20.7	53	49.4	10.6	60.0
12	HPAM	41	33	30.0	4.5	87.0	21.1	49	52.9	9.2	62.1

Note: η_1 and η_2 are the viscosity of displacing fluids (2000 mg·L^{-1}) at 25 °C and 45 °C, respectively; l is the edge length of the rectangular prismatic core sample.

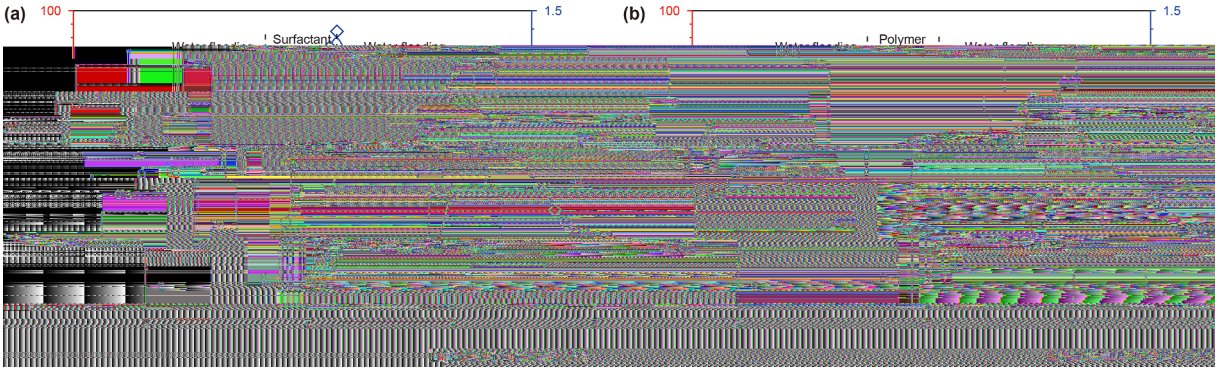

i Oil recovery factor and displacement pressure of the displacing fluid plotted versus injection volume. ( ) 2000 mg·L^{-1} EDAB solution; (●) 2000 mg·L^{-1} HPAM solution. TDS, 4500 mg·L^{-1} NaCl; T, 45 °C.

enhancement of 10.6% in ultimate recovery (Fig. 11(a)). For the HPAM solution, both the pressure profile and oil recovery curve exhibited trends analogous to those observed with EDAB. The initial water flooding recovery factor stabilized at 52.9%, while the polymer flooding yielded an incremental recovery of 9.2% (Fig. 11 (b)). As further delineated in Table 4, HPAM demonstrates higher initial injection viscosity than EDAB. Significantly, at the experimental temperature of 45 °C, EDAB exhibits superior viscosity retention alongside a 1.4% advantage in enhanced oil recovery over HPAM. This integrated performance profile mechanistically validates enhanced displacement efficacy of EDAB.

Conclusions

In summary, this study identifies EDAB as a promising viscoelastic surfactant alternative to conventional HPAM for EOR application in Daqing Oilfield. Our systematic evaluation demonstrates superior thermal stability, robust salt tolerance, and improved interfacial activity of EDAB. Notably, EDAB shows distinct thermo-thickening behavior—its viscosity increases by 89% over the temperature range of 25–55 °C, which aligns precisely with the temperature variation experienced by displacement fluids during injection (surface to bottomhole) and transport in porous media. Unlike HPAM, which typically suffers viscosity loss under such conditions, the viscosity of EDAB increases with temperature, offering a highly desirable performance for displacement fluids.

Additionally, EDAB demonstrates exceptional salt tolerance, retaining nearly 100% of its viscosity even at Ca^{2+} and Mg^{2+} concentrations of 80 mg/L, far surpassing HPAM's 63.5% retention. It also achieves significant IFT reduction, reaching 10^{-2} mN·m^{-1} at just 2000 mg·L^{-1}. Core-flooding tests further confirm its EOR potential, with a 10.6% incremental recovery (compared to HPAM's 9.2%) due to improved sweep efficiency and oil/water interfacial activity.

These findings position EDAB as a viable solution for EOR in saline environments where conventional EOR polymers underperform. Moving forward, research efforts should prioritize optimizing EDAB for field-scale applications, with particular attention to its interactions under varying reservoir conditions to maximize recovery efficiency and minimize adsorption losses. Additionally, enhancing EDAB's temperature and salt resistance will be crucial for extending its applicability to high-temperature, high-salinity reservoirs. Finally, developing a cost-effective and scalable synthesis method will be essential to facilitate EDAB's practical adoption in real-world settings.

CRediT authorship contribution statement

[illegible]: Writing – original draft, Methodology, Investigation, Data curation. **[illegible]:** Methodology, Investigation, Data curation. **[illegible]:** Validation, Resources. **[illegible]:** Validation, Resources. **[illegible]:** Methodology, Formal analysis. **[illegible]:** Writing – review & editing, Supervision, Project administration, Methodology. **[illegible]:** Writing – review & editing, Supervision, Project administration, Funding acquisition, Conceptualization.

Declaration of competing interest

The authors declare that they have no known competing financial interests or personal relationships that could have appeared to influence the work reported in this paper.

[illegible]

This work was supported by the Key Joint Fund of National Natural Science Foundation of China (U23B2085) and China National Petroleum Corporation Innovation Fund (2022DQ02-0205).

Appendix [illegible]

Supplementary data to this article can be found online at https://doi.org/10.1016/j.petsci.2025.08.007.

References

Abdelgawad, K.Z., 2022. Polymer induced permeability reduction: The influence of polymer retention and porous medium properties. J. Petrol. Sci. Eng. 217, 110821. https://doi.org/10.1016/j.petrol.2022.110821.

Ahmed, M.E., Sultan, A.S., Al-Sofi, A., Al-Hashim, H.S., 2023. Optimization of surfactant-polymer flooding for enhanced oil recovery. J. Pet. Explor. Prod. Technol. 13, 2109–2123. https://doi.org/10.1007/s13202-023-01651-0.

Agharazi-Dormani, N., Hornof, V., Neale, G.H., 1990. Effects of divalent ions in surfactant flooding. J. Petrol. Sci. Eng. 4 (3), 189–196. https://doi.org/10.1016/0920-4105(90)90008-Q.

Akstinat, M.H., 1980. Polymes for enhanced oil recovery in reservoirs of extremely high salinities and high temperatures. In: SPE International Symposium on Oilfield and Geothermal Chemistry. https://doi.org/10.2118/8979-MS.

Al-Asadi, A., Somoza, A., Arce, A., Rodil, E., Soto, A., 2023. Nanofluid based on 1-dodecylpyridinium chloride for enhanced oil recovery. Pet. Sci. 20 (1), 600–610. https://doi.org/10.1016/j.petsci.2022.08.018.

Ameli, F., Moghbeli, M.R., Alashkar, A., 2019. On the effect of salinity and

Dreiss, C.A., 2007. Wormlike micelles: Where do we stand? Recent developments, linear rheology and scattering techniques. Soft Matter 3 (8), 956–970. https://doi.org/10.1039/B705775J.
Doe, P.H., Moradi-Araghi, A., Shaw, J.E., Stahl, G.A., 1987. Development and evaluation of EOR polymers suitable for hostile environments—Part 1: copolymers of vinylpyrrolidone and acrylamide. SPE Reserv. Eng. 2 (4), 461–467. https://doi.org/10.2118/1